Constraining the pseudo-Dirac nature of neutrinos using astrophysical neutrino flavor data

Chee Sheng Fong[*] and Yago Porto[†]

Centro de Ciências Naturais e Humanas, Universidade Federal do ABC, 09.210-170, Santo André, São Paulo, Brazil

(Received 1 August 2024; accepted 1 August 2025; published 3 September 2025)

The three Standard Model neutrinos can have Majorana mass or strictly Dirac mass, but both scenarios are practically indistinguishable in neutrino oscillation experiments. If they are pseudo-Dirac, however, there will be new mass splittings among the pseudo-Dirac pairs, potentially leaving traces in neutrino oscillation phenomena. In this work, we use flavor ratios of astrophysical neutrinos to discriminate different possible mass spectra of pseudo-Dirac neutrinos. We show that it will be possible to impose robust bounds of order $\delta m_3^2 \lesssim 10^{-12}$ eV^2 on the new mass squared splitting involving the third pseudo-Dirac mass eigenstates (those with the least electron flavor composition) with the future experiment IceCube-Gen2. The derived sensitivity is robust because it only assumes an extragalactic origin for the astrophysical neutrinos and hierarchical pseudo-Dirac mass spectrum. In case the neutrino sources are known in the future, such bounds can potentially improve by up to five orders of magnitude, reaching $\delta m_3^2 \lesssim 10^{-17}$ eV^2.

DOI: 10.1103/yc27-61w5

I. INTRODUCTION

Nonzero neutrino mass with at least one mass eigenstate with a mass of greater than 0.05 eV has been established experimentally through neutrino oscillation phenomena [1,2]. In the Standard Model (SM), neutrinos, being electrically neutral, are the only fermions that can acquire Majorana mass without breaking the electromagnetic gauge symmetry. To respect the full SM gauge symmetry, Majorana neutrino mass can only arise from new physics at some scale Λ which breaks the total lepton number by two units. This leads to neutrinoless double beta decay, which, in the case of an inverted neutrino mass ordering scenario, should be observable in future experiments such as nEXO [3]. On the other hand, if neutrinos were to have Dirac mass, new fermion degrees of freedom (the right-handed neutrinos) have to be introduced.

In this case, since the lepton number is conserved, the neutrinoless double beta decay signature will be absent. In neutrino foscillation experiments where the lepton number is conserved, one cannot distinguish between Majorana and Dirac neutrinos. However, if the lepton number is slightly broken such that neutrinos are pseudo-Dirac, there will be a new small mass splitting among the pseudo-Dirac pair.[1] While the rate of neutrinoless double beta decay will be suppressed due to small lepton number violation, interestingly, one can probe this scenario in neutrino oscillation experiments as we will discuss next.

In the pseudo-Dirac scenario [7], we can have up to three pairs of mass eigenstates ($i = 1, 2, 3$) with squared masses,

$$\hat{m}_j^2 = m_j^2 - \frac{1}{2}\delta m_j^2, \qquad \hat{m}_{j+3}^2 = m_j^2 + \frac{1}{2}\delta m_j^2, \tag{1}$$

where m_j^2 are the standard mass squared eigenvalues and δm_j^2 are the three new mass squared splittings which have not been observed experimentally and are expected to be smaller than the solar mass splitting. Due to the pseudo-Dirac structure, the mixing between the SM and the right-handed neutrinos are close to maximal. Under the assumption of maximal mixing, strong experimental constraints using solar neutrino data have been derived: $\delta m_{1,2}^2 \lesssim 10^{-11}$ eV^2, while it is not sensitive to δm_3^2 due to small θ_{13} [4,8–10]. (See also [11].) Using atmospheric, beam and reactor neutrino data which are sensitive to atmospheric mass splitting and θ_{13}, a much weaker constraint is obtained $\delta m_3^2 \lesssim 10^{-5}$ eV^2 [4]. (See also [8].) Due to the small mass splitting, astrophysical neutrinos coming from distance sources of Mpc to Gpc allow one to probe a

[*]Contact author: sheng.fong@ufabc.edu.br
[†]Contact author: yago.porto@ufabc.edu.br

Published by the American Physical Society under the terms of the Creative Commons Attribution 4.0 International license. Further distribution of this work must maintain attribution to the author(s) and the published article's title, journal citation, and DOI. Funded by SCOAP[3].

[1]The same scenario is referred to as quasi-Dirac in Refs. [4–6] but we will opt for pseudo-Dirac, which is a more popular choice in the literature.

mass squared difference much smaller than 10^{-12} eV^2 [8,12–23]. While the pseudo-Diracness of neutrinos is interesting in itself, Ref. [6] has showed that it could be linked to the cosmic baryon asymmetry for the pseudo-Dirac seesaw model where the new squared mass splitting is intimately connected to the CP violation ϵ required for baryogenesis through leptogenesis as follows[2]:

$$\delta m_i^2 \gtrsim 10^{-8}\ \text{eV}^2 \left(\frac{m_i}{0.1\ \text{eV}}\right)^2 \left(\frac{\epsilon}{10^{-7}}\right). \tag{2}$$

Here $\epsilon \sim 10^{-7}$ represents roughly the minimum value required to explain the observed baryon asymmetry. Given current constraints, this can only be achieved by δm_3^2. This provides further motivation to explore the third pseudo-Dirac mass splitting within this range.

The advent of neutrino telescopes made it possible to study neutrino properties using high-energy (HE) astrophysical neutrinos [25]. Neutrino telescopes employ naturally occurring targets with large volumes to detect tiny astrophysical neutrino fluxes amidst the overwhelming backgrounds of atmospheric neutrinos and muons [26]. The IceCube Neutrino Observatory, for instance, has utilized a cubic kilometer of Antarctic ice since 2011 to observe neutrinos in the TeV–PeV range [27]. Following the discovery of HE neutrinos in 2013 [28,29], further observations by IceCube [30–36], ANTARES [37], and Baikal-GVD [38] initiated an ongoing phase of characterizing the diffuse neutrino flux and searching for candidate neutrino sources [39–43]. However, despite the recent identification of the first neutrino sources in the northern hemisphere, the origins of most of the diffuse flux are still unknown [44,45], and the absence of strong anisotropies in the flux indicates an extragalactic origin, with a minor galactic contribution at the level of 10% [46–48].

The extragalactic origin of the HE neutrinos suggests that these particles travel, from their production to detection, a minimum distance of $L \approx 15$ kpc, equivalent to the radius of the Milky Way Galaxy. This estimate is notably conservative, considering that the Andromeda Galaxy, the closest major galaxy, lies 600 kpc away, while the nearest active galactic nucleus (NGC5128) is situated roughly 4 Mpc from the Milky Way. This estimate is also compatible with the redshift evolution of BL Lac objects [49,50]. The important quantity which allows pseudo-Dirac neutrinos to be constrained is the pseudo-Dirac oscillating phase $\Phi_j \sim \delta m_j^2 L/E$. If $\Phi_j \ll 1 \Rightarrow \delta m_j^2 \ll E/L$; the pseudo-Dirac pair remains coherent throughout the propagation and the oscillation approaches the standard scenario and we lose the sensitivity to constrain the scenario. If $\Phi_j \gg 1$, we have the *decoherence* among the pseudo-Dirac pair and since sterile states are not detected, the corresponding probability amplitude is suppressed by a factor of 2. Even with a conservative choice of $L \sim 15$ kpc, under the assumption of hierarchical pseudo-Dirac mass splittings, we anticipate that IceCube-Gen2 [51] should be able to impose the constraint $\delta m_3^2 \lesssim 10^{-12}$ eV^2 due to its improved flavor ratio measurements [52]. This will leverage the constraint on δm_3^2 to the level of the current constraints on $\delta m_{1,2}^2$. On the other hand, in the more optimistic scenario where most potential neutrino sources reside farther away, for example at $z \sim 1$, as suggested by the star-formation rate [50,53], the bounds would improve: $\delta m_3^2 \lesssim 10^{-17}$ eV^2.

In this work, we will use astrophysical neutrino flavor ratios and the decoherence condition $\Phi_j \gg 1$ to probe pseudo-Dirac neutrinos [12–14,17,18,54,55]. In this approach, insensitivity to absolute neutrino flux is a double-edged sword. The advantage is that when there exist hierarchies between δm_i^2, irrespective of spectral feature, capitalizing on the decoherence effect, stringent upper bounds on larger δm_i^2 can be derived as we will show in this work. The disadvantage is that if all δm_i^2 ($i = 1, 2, 3$) are of the same order, we will lose the sensitivity since the transition probabilities for all flavors get approximately the same suppression. This is to be compared with studies which consider specific astrophysical sources where only certain ranges of δm_i^2 for the first few oscillations can be probed and, away from this region, the analysis is limited by absolute flux uncertainty and knowledge of the spectral feature [19–23]. If the flux from certain source can be determined quite accurately, and in particular, if all δm_i^2 are of the same order, this latter approach is superior. In the view that only very few astrophysical neutrino sources are identified, we will focus on the flavor ratios approach and see how well this will fare.

The paper is organized as follows: In Sec. II, we will review the parametrization of the pseudo-Dirac model at low energy while in Sec. III, we will discuss the framework to calculate the oscillation probability in this scenario. Then, we will present our main results in Sec. IV and conclude in Sec. V. In the Appendix, we investigate the effects of varying astrophysical neutrino sources.

II. PSEUDO-DIRAC MODEL

If all three SM neutrinos ν_α ($\alpha = e, \mu, \tau$) are pseudo-Dirac in nature, we need to introduce the corresponding right-handed neutrinos ν'_α. (While we have used the same index α, the flavors of ν'_α are arbitrary since they do not feel the SM weak interaction.) After the electroweak symmetry breaking, we can write down the effective neutrino mass term as $\overline{\Psi^c}\mathcal{M}\Psi$ for $\Psi \equiv (\nu_e, \nu_\mu, \nu_\tau, \nu'_e, \nu'_\mu, \nu'_\tau)^T$ with

$$\mathcal{M} = \begin{pmatrix} m_M & m_D \\ m_D^T & m'_M \end{pmatrix}, \tag{3}$$

[2]The pseudo-Dirac leptogenesis model proposed in Ref. [24] does not impose such a strong constraint, predicting only a lower bound on seesaw scale for a given pseudo-Dirac mass splitting.

where the total lepton number is conserved by the Dirac mass term m_D but broken by the Majorana mass terms m_M, m'_M. Without loss of generality, we can work in the basis where the charged lepton Yukawa is real and diagonal. We define the pseudo-Dirac scenario as when the matrix entries satisfying

$$|m_M|, |m'_M| \ll |m_D|, \tag{4}$$

where the total lepton number is slightly broken.

Let us first look at the Dirac limit $m_M, m'_M \to 0$ where the total lepton number is exactly conserved. In this case, m_D can be diagonalized by two unitary matrices U_0 and V_0 as follows:

$$\hat{m} = U_0^T m_D V_0 = \mathrm{diag}(m_1, m_2, m_3). \tag{5}$$

Defining

$$\mathcal{U} = \frac{1}{\sqrt{2}} \begin{pmatrix} U_0 & iU_0 \\ V_0 & -iV_0 \end{pmatrix}, \tag{6}$$

$\mathcal{M}$ can be diagonalized as $\mathcal{U}^T \mathcal{M} \mathcal{U} = \mathrm{diag}(\hat{m}, \hat{m})$ where the mass eigenstates are given by

$$\hat{\Psi} = \mathcal{U}^\dagger \Psi \equiv (\nu_1, \nu_2, \nu_3, \nu'_1, \nu'_2, \nu'_3)^T. \tag{7}$$

We can also express the flavor eigenstates in terms of the mass eigenstates as

$$\Psi = \mathcal{U}\hat{\Psi} = \frac{1}{\sqrt{2}} \begin{pmatrix} U_0(\nu + i\nu') \\ V_0(\nu - i\nu') \end{pmatrix}, \tag{8}$$

where $\nu \equiv (\nu_1, \nu_2, \nu_3)^T$ and $\nu' \equiv (\nu'_1, \nu'_2, \nu'_3)^T$ pair up to form three Dirac states (*maximal* mixing). Experimentally, only ν_α participate in weak interactions, and hence only U_0 can be measured.

When $m_M, m'_M \neq 0$ but the pseudo-Dirac condition (4) is still satisfied, there will be deviation from Eq. (6) and we will have three pairs of pseudo-Dirac mass eigenstates with masses ($j = 1, 2, 3$)

$$\hat{m}_j = m_j - \delta m_j, \qquad \hat{m}_{j+3} = m_j + \delta m_j. \tag{9}$$

A useful Euler parametrization for unitary matrix $\mathcal{U}$ is given by

$$\mathcal{U} = \frac{1}{\sqrt{2}} \begin{pmatrix} AU_0 + B & i(AU_0 - B) \\ CU_0 + D & i(CU_0 - D) \end{pmatrix}, \tag{10}$$

where U_0 is a 3×3 unitary matrix while the rest of the 3×3 matrices A, B, C, and D are constrained by $\mathcal{U}\mathcal{U}^\dagger = \mathcal{U}^\dagger \mathcal{U} = I_{3\times 3}$. For example, from $\mathcal{U}\mathcal{U}^\dagger = I_{3\times 3}$, we have

$$AA^\dagger + BB^\dagger = CC^\dagger + DD^\dagger = I_{3\times 3}, \tag{11}$$

$$AC^\dagger + BD^\dagger = CA^\dagger + DB^\dagger = 0. \tag{12}$$

In the Dirac limit, $A = I_{3\times 3}$, $B = C = 0$, and $D = V_0$ and Eq. (6) is recovered. Explicitly, we can construct the mixing matrix as

$$\mathcal{U} = U_{\mathrm{new}} U Y,$$

where

$$U_{\mathrm{new}} = R_{56} R_{46} R_{36} R_{26} R_{16} R_{45} R_{35} R_{25} R_{15} R_{34} R_{24} R_{14},$$
$$U = R_{23} R_{13} R_{12},$$

and

$$Y \equiv \frac{1}{\sqrt{2}} \begin{pmatrix} I_{3\times 3} & iI_{3\times 3} \\ I_{3\times 3} & -iI_{3\times 3} \end{pmatrix},$$

with R_{ij} the complex rotation matrix in the ij plane which can be obtained from a 6×6 identity matrix I by replacing the I_{ii} and I_{jj} by $\cos\theta_{ij}$, I_{ij} by $e^{-i\phi_{ij}} \sin\theta_{ij}$ and I_{ji} by $e^{i\phi_{ij}} \sin\theta_{ij}$. To recover the Dirac limit, we set all the angles in U_{new} (besides θ_{45}, θ_{46}, θ_{56}) to zero. The new angles θ_{45}, θ_{46}, θ_{56} which describe the mixing among the sterile neutrinos (through V_0 in the Dirac limit) are in principle not measurable through the SM interactions.

While the deviation from maximal mixing U_0 is of the order of the following ratios of matrix entries,

$$\delta U_0 \sim \frac{|m_M|}{|m_D|}, \frac{|m'_M|}{|m_D|}, \tag{13}$$

the pseudo-Dirac mass squared splittings are of the order of $\delta m_j^2 \sim m_j^2 \delta U_0$. For example, taking $m_j \sim 0.1$ eV and $\delta U_0 \sim 10^{-4}$, the new mass splitting is $\delta m_j^2 \sim 10^{-6}$ eV^2. So, it is expected that the first discovery of pseudo-Diracness should be through the new mass splittings. In this study, we will assume maximal mixing and focus only on the effects of new mass splittings. We will leave the consideration of deviation from maximal mixing for future study.

III. OSCILLATION PROBABILITY

The amplitude of a neutrino of flavor state ν_α created at $t = 0$ being detected as ν_β at time $t > 0$, $S_{\beta\alpha}(t) \equiv \langle \nu_\beta | \nu_\alpha(t) \rangle$ satisfies the Schrödinger equation

$$i\frac{d}{dt} S(t) = HS(t). \tag{14}$$

The Hamiltonian in the flavor basis is given by

$$H = \mathcal{U}\Delta\mathcal{U}^\dagger + V, \tag{15}$$

where $\mathcal{U}$ is the leptonic mixing matrix, $\Delta \equiv \mathrm{diag}(\hat{m}_1^2, \hat{m}_2^2, \ldots)/(2E)$ with E the neutrino energy, and V is the matter potential. For the pseudo-Dirac model discussed in the previous section, assuming that the ν'_α has no new interactions with the SM, the matter potential for ordinary matter is $V = \mathrm{diag}(V_e - V_n, -V_n, -V_n, 0, 0, 0)$ with $V_e = \sqrt{2}G_F n_e$ and $V_n = G_F n_n/\sqrt{2}$ where G_F is the Fermi constant, and, n_e and n_n are the electron and neutron number density, respectively. The solution to Eq. (14) is formally given by

$$S = T\ \exp\left[-i\int_0^t dt' H(t')\right], \tag{16}$$

where T denotes time ordering.

For astrophysical neutrinos, even if the matter effect is negligible, there is still nontrivial time dependence due to cosmic expansion. Defining the redshift z as

$$1 + z \equiv \frac{a_0}{a}, \tag{17}$$

where a is the cosmic scale factor with a_0 the value today, we have

$$dt = \frac{dt}{da}da = -\frac{dz}{(1+z)\mathcal{H}}, \tag{18}$$

where $\mathcal{H} \equiv \frac{1}{a}\frac{da}{dt}$ is the Hubble expansion rate which can be expressed in terms of the current expansion rate $\mathcal{H}_0$, total matter fraction Ω_m, and dark energy fraction Ω_Λ as follows:

$$\mathcal{H}(z) = \mathcal{H}_0\sqrt{\Omega_m(1+z)^3 + \Omega_\Lambda}. \tag{19}$$

In the above, we have ignored the small radiation density and from the measurements of the Planck satellite, we have $\Omega_m = 0.315$, $\Omega_\Lambda = 0.685$, and $\mathcal{H}_0 = 67.4\ \mathrm{km\,s^{-1}\,Mpc^{-1}}$ [56]. Furthermore, the energy of the neutrino E detected at $z = 0$ will be equal to $E(1+z)$ at redshift $z > 0$. With negligible matter effect for astrophysical neutrinos $V = 0$, we can write the solution as

$$S_{\beta\alpha} = \sum_j \mathcal{U}_{\beta j}\mathcal{U}^*_{\alpha j} e^{-i\frac{m_j^2}{2E}L_{\mathrm{eff}}}, \tag{20}$$

where we have defined the effective distance as

$$L_{\mathrm{eff}} \equiv c\int_0^z \frac{dz'}{(1+z')^2\mathcal{H}(z')}, \tag{21}$$

with the speed of light c shown explicitly due to the unit of $\mathcal{H}_0$ that we have chosen. For $z < 1$, we can Taylor expand in z and obtain at the leading order

$$L_{\mathrm{eff}} \simeq \frac{cz}{\mathcal{H}_0} = 4.4\ \mathrm{Mpc}\left(\frac{z}{0.001}\right)\left(\frac{67.4\,\mathrm{km\,s^{-1}\,Mpc^{-1}}}{\mathcal{H}_0}\right), \tag{22}$$

where the corrections are $\mathcal{O}(z^2)$. Finally, the transition probability is given by the Born rule $P(\nu_\alpha \to \nu_\beta) \equiv |S_{\beta\alpha}|^2$.

Assuming the new angles are negligible but new mass splittings are relevant, we have the oscillation probability

$$P(\nu_\alpha \to \nu_\beta) = \left|\sum_{j=1}^3 U_{0,\beta j}U^*_{0,\alpha j} e^{-i\frac{m_j^2}{2E}L_{\mathrm{eff}}}\cos(\Phi_j)\right|^2, \tag{23}$$

where we have defined

$$\Phi_j \equiv \frac{\delta m_j^2}{4E}L_{\mathrm{eff}}, \tag{24}$$

and used $\delta m_j^2 \simeq 4m_j\delta m_j$ from the definitions in Eqs. (1) and (9). Astrophysical neutrino sources are far enough such that we can average out all the standard oscillations involving $m_j^2 - m_k^2 \neq 0$ and obtain

$$P(\nu_\alpha \to \nu_\beta) \simeq \sum_{j=1}^3 |U_{0,\beta j}U^*_{0,\alpha j}|^2\cos^2(\Phi_j). \tag{25}$$

If all δm_j^2 are also large enough

$$\Phi_j = 10\left(\frac{\delta m_j^2}{1.7\times10^{-12}\ \mathrm{eV}^2}\right)\left(\frac{L_{\mathrm{eff}}}{15\ \mathrm{kpc}}\right)\left(\frac{100\ \mathrm{TeV}}{E}\right) \gg 1, \tag{26}$$

such that we can average out these new oscillations, we obtain

$$P(\nu_\alpha \to \nu_\beta) \simeq \frac{1}{2}\sum_{j=1}^3 |U_{0,\beta j}U^*_{0,\alpha j}|^2. \tag{27}$$

In general, Eq. (27) changes the flux normalization for all flavors. However, if the absolute flux is unknown, it will be challenging to distinguish it from the standard scenario.

On the other hand, using neutrino flavor ratios which do not depend on absolute flux, one can distinguish between the following six cases: Case 1, Case 2, Case 3, Case 12, Case 23, and Case 13 where Case j is defined as $\delta m^2_{k\neq j} = 0$ and $\Phi_j \gg 1$ with oscillation probability

$$P^j_{\alpha\beta} \equiv \frac{1}{2}|U_{0,\beta j}U^*_{0,\alpha j}|^2 + \sum_{k\neq j}|U_{0,\beta k}U^*_{0,\alpha k}|^2, \tag{28}$$

and Case jk is defined as $\delta m^2_{l\neq\{j,k\}} = 0$ and $\Phi_{j,k} \gg 1$ with oscillation probability

$$P^{jk}_{\alpha\beta} \equiv \frac{1}{2}|U_{0,\beta j}U^*_{0,\alpha j}|^2 + \frac{1}{2}|U_{0,\beta k}U^*_{0,\alpha k}|^2 + \sum_{l\neq\{j,k\}} |U_{0,\beta l}U^*_{0,\alpha l}|^2. \tag{29}$$

By $\delta m^2_{k\neq j} = 0$, we mean $\delta m^2_{k\neq j} \ll \delta m^2_j$ such that oscillations involving $\delta m^2_{k\neq j}$ have not developed. For example, considering the most distant identified source of astrophysical neutrinos PKS $1424+240$ of 2.6 Gpc together with $E = 1$ TeV [22,57], we need $\delta m^2_{k\neq j} \ll 10^{-20}$ eV^2 such that the oscillation involving $\delta m^2_{k\neq j}$ has not developed. Since very few astrophysical neutrino sources have been identified, the best we can currently do is to make assumptions based on the six possible scenarios mentioned above.

The relevant dataset of high-energy starting events (HESE) [35], from which neutrino flavors can be distinguished by IceCube, includes events with energies above 60 TeV and up to approximately 10 PeV. According to Eq. (26), the corresponding sensitivity range of pseudo-Dirac mass splittings for our analysis is shown for each case in Table I. For example, in Case 3, where the expected regions for the standard and pseudo-Dirac scenarios do not overlap significantly (see next section), if the data remains consistent with the standard scenario at a given confidence level, we can place an upper bound on the mass splitting, $\delta m^2_3 \lesssim 10^{-10}$ eV^2, assuming $\delta m^2_{1,2} = 0$. This bound corresponds to the decoherence condition set by the upper end of the energy window, approximately 10 PeV. More stringent upper bounds, however, can be obtained by using lower-energy neutrinos around 100 TeV, for which the decoherence condition in Eq. (26) implies $\delta m^2_3 \lesssim 10^{-12}$ eV^2. Statistically, this latter bound is expected to dominate (and is the one quoted in Table I), as lower-energy neutrinos yield higher event statistics [35].

A. Neutrino flavor ratios

In the standard scenario, the oscillation probability between an initial flavor ν_α to a final flavor ν_β is given by

$$P^{std}_{\alpha\beta} = \sum_{i=1}^{3} |U_{\alpha i}|^2 |U_{\beta i}|^2. \tag{30}$$

Therefore, for a flavor composition $(f_{e,S}, f_{\mu,S}, f_{\tau,S})$ at the source S, we can compute the final flavor at Earth as

$$f_{\beta,\oplus} = \sum_{\alpha=e,\mu,\tau} P^{std}_{\alpha\beta} f_{\alpha,S}. \tag{31}$$

In the presence of averaged-out pseudo-Dirac oscillations, we must change $P^{std}_{\alpha\beta}$ to $P^{j}_{\alpha\beta}$ or $P^{jk}_{\alpha\beta}$, where the indices j and jk correspond to the pseudo-Dirac scenarios described by Eqs. (28) and (29). Therefore, for such cases, the final fractions of active flavors ν_β are given by $f^{j}_{\beta,\oplus} = \sum_\alpha P^{j}_{\alpha\beta} f_{\alpha,S}$ and $f^{jk}_{\beta,\oplus} = \sum_\alpha P^{jk}_{\alpha\beta} f_{\alpha,S}$, respectively. However, due to the finite conversion probability between active and sterile states, the total flux of active neutrinos will not be conserved from production to detection. Therefore, to determine the detected fractions, we need to normalize $f^{j}_{\beta,\oplus}$ and $f^{jk}_{\beta,\oplus}$:

$$f^{j,\mathrm{det}}_{\beta,\oplus} = \frac{f^{j}_{\beta,\oplus}}{f^{j}_{e,\oplus} + f^{j}_{\mu,\oplus} + f^{j}_{\tau,\oplus}} \quad \text{and}$$
$$f^{jk,\mathrm{det}}_{\beta,\oplus} = \frac{f^{jk}_{\beta,\oplus}}{f^{jk}_{e,\oplus} + f^{jk}_{\mu,\oplus} + f^{jk}_{\tau,\oplus}}. \tag{32}$$

Next, we will focus on the aforementioned six cases and evaluate the sensitivity of IceCube and IceCube-Gen2 in constraining/distinguishing them.

TABLE I. The cases with their corresponding pseudo-Dirac mass splitting ranges are valid for any astrophysical neutrinos with $E \sim 100$ TeV from extragalactic sources i.e. $L > 15$ kpc. The meaning of $\delta m^2_j = 0$ can be taken to be $\delta m^2_j \ll 10^{-20}$ eV^2 considering the most distant identified astrophysical neutrino source (see text for discussion).

Case	Pseudo-Dirac mass splitting
Case 1	$\delta m^2_1 \gtrsim 10^{-12}$ eV^2, $\delta m^2_{2,3} = 0$
Case 2	$\delta m^2_2 \gtrsim 10^{-12}$ eV^2, $\delta m^2_{1,3} = 0$
Case 3	$\delta m^2_3 \gtrsim 10^{-12}$ eV^2, $\delta m^2_{1,2} = 0$
Case 12	$\delta m^2_{1,2} \gtrsim 10^{-12}$ eV^2, $\delta m^2_3 = 0$
Case 23	$\delta m^2_{2,3} \gtrsim 10^{-12}$ eV^2, $\delta m^2_1 = 0$
Case 13	$\delta m^2_{1,3} \gtrsim 10^{-12}$ eV^2, $\delta m^2_2 = 0$

IV. RESULTS

HE astrophysical neutrinos are generated in cosmic particle accelerators when accelerated protons collide with matter (pp interactions) and radiation ($p\gamma$ interactions) [58–62]. These collisions produce mesons, particularly charged pions ($\pi^\pm$), which then decay into neutrinos. The decay chain $\pi^- \to \mu^- + \bar{\nu}_\mu \to e^- + \bar{\nu}_e + \nu_\mu + \bar{\nu}_\mu$, along with its charge conjugate reaction, produces two muon neutrinos for every electron neutrino: $(1,2,0)_S$, where the subscript S denotes the initial proportions at the source.[3] It is also possible that the decay chain described above is not complete, as the muon may lose energy due to synchrotron emission before decaying. As a result, this will generate the μ-damped scenario, with the proportions $(0,1,0)_S$ [68–72]. In this section, however, we assume neutrinos are produced only by the complete chain

[3]Neutrinos and antineutrinos cannot be distinguished at the IceCube detector. The only exception is the Glashow resonance [63–66], but it suffers from a lack of statistics, with only one candidate event detected so far [67].

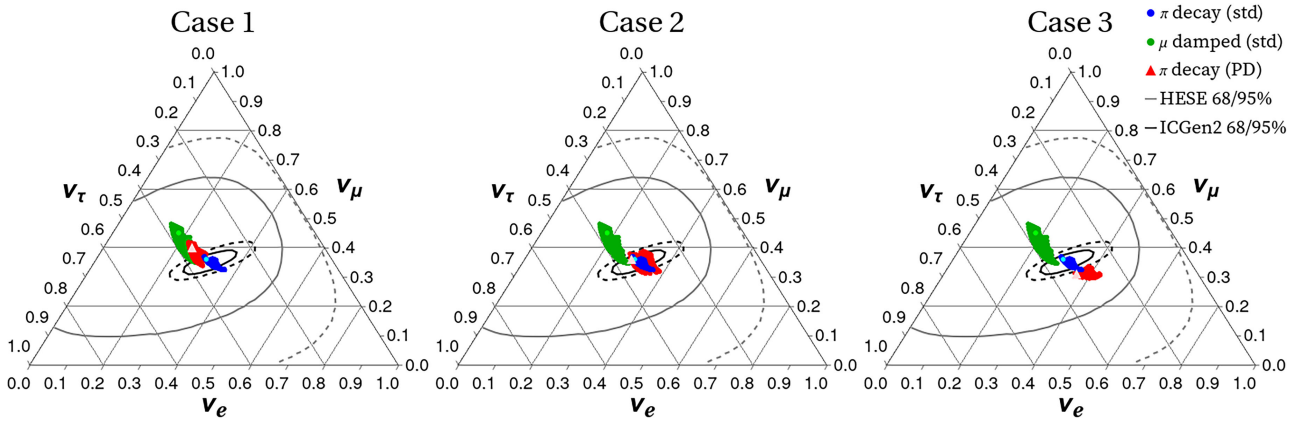


FIG. 1. Expected regions for the flavor composition of HE astrophysical neutrinos, considering the 3σ interval for the oscillation parameters in [1], valid for both normal and inverted mass orderings. The standard (std) expectation for π decay is shown in blue, the standard μ damped expectation is shown in green, and the various scenarios for pseudo-Dirac neutrinos are shown in red. In Case j, oscillations corresponding to pseudo-Dirac squared mass splitting δm_j^2 have been averaged out. See the text for more details about the different pseudo-Dirac scenarios.

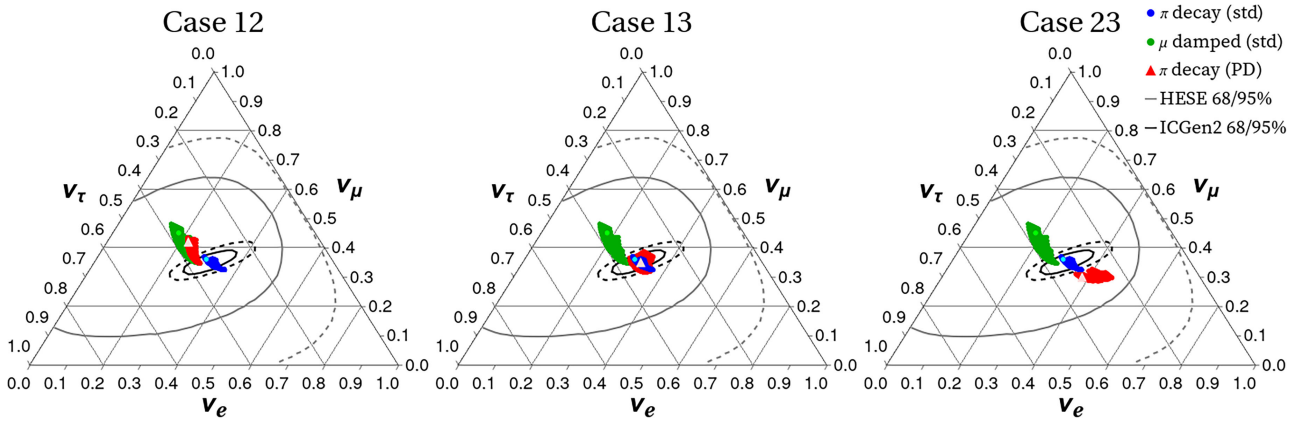


FIG. 2. Same as Fig. 1 but for pseudo-Dirac scenarios named Case jk.

of $\pi^\pm$ decay and reach Earth with averaged-out pseudo-Dirac oscillations, as described by Eqs. (28) and (29), and compare these scenarios with the standard expectations for both π decay and μ damped. More information regarding the μ-damped production combined with the pseudo-Dirac scenario is reserved for the Appendix.

During propagation from the sources to Earth, neutrino oscillations modify the initial flavor proportions. In the standard vacuum oscillation scenario, assuming the absence of matter effects [73] and pseudo-Dirac mass splittings, the $\pi^\pm$ production channel results in flavor equipartition at Earth: $(1:2:0)_S \to (1:1:1)_\oplus$. To be more precise, in Figs. 1 and 2, we show the allowed region for the flavor composition at Earth after considering the 3σ uncertainties of the oscillation parameters [1] where there is no perceptible distinction between normal and inverted mass orderings. Due to the smallness of $\sin\theta_{13}$, the effect of the leptonic CP phase $\delta_{\rm CP}$ on the allowed region is small; for this reason and to be as conservative as possible, we do not take into account the correlation between θ_{23} and $\delta_{\rm CP}$. Observe that the π decay (blue region) using the best fit oscillation parameters of Ref. [1], in the standard case, is given by $(0.3, 0.36, 0.34)_\oplus$, which lies very close to the benchmark of total flavor equipartition. On the other hand, for the μ-damped case (green region), the best fit is $(0.18, 0.45.0.37)_\oplus$. Also represented in Figs. 1 and 2 are the regions corresponding the neutrino flavor at Earth in the presence of averaged-out pseudo-Dirac oscillation as described by Eqs. (28) and (29) (red regions). We investigate all possible cases listed in Sec. III.

We observe that Case 3 and Case 23 stand out as the most distinct from the standard scenarios, even when considering the current uncertainties in the oscillation parameters and production processes (π decay or μ damped). What makes the regions corresponding to Cases 3 and 23 so distinct from the standard scenarios is that by decreasing the amount of ν_3 in the flux, we automatically reduce the

proportion of $f_{\mu,\oplus}$[4] (as well as $f_{\tau,\oplus}$, but in a smaller quantity), due to the larger mixing of this propagation eigenstate with ν_μ. Applying the same reasoning, if some of the ν_1 eigenstates disappear (Case 1 or Case 12), $f_{e,\oplus}$ decreases, and the expected region shifts closer to the typical μ-damped scenario. For Case 13, however, the decrease of $f_{\mu,\oplus}$ due to the disappearance of ν_3 is balanced by the decrease in $f_{e,\oplus}$ resulting from the disappearance of ν_1, making the final region compatible with the standard π decay. Moreover, ν_2 has roughly equal mixing with all flavors, so its disappearance (Case 2) has a smaller effect. These results hold true for both normal and inverted mass orderings.

Figures 1 and 2 also show the 68% and 95% C.L. contours corresponding to the IceCube analysis [34] of the flavor composition of the HE astrophysical neutrinos using the HESE sample [35]. HESE is an all-flavor, all-sky search using 7.5 yrs of IceCube data for neutrinos with energies above 60 TeV. Observe that we cannot draw any conclusions from the current HESE bounds, which are still too weak to discriminate even between the standard scenarios. Nevertheless, future detectors, such as IceCube-Gen2 [51], with more statistics and improved capabilities, might significantly enhance the sensitivity to the flavor composition. In Figs. 1 and 2 we also show the 68% and 99% projected sensitivities of IceCube-Gen2 after 10 yrs of observations. The projection of IceCube-Gen2 is taken from [52] and assumes the best fit value to be $(0.3, 0.36, 0.34)_\oplus$, compatible with standard π decay. Observe that with IceCube-Gen2, we can start to distinguish between the standard scenario and some pseudo-Dirac scenarios (Case 3 and Case 23), even if the production process (π decay and/or μ damped) remains uncertain at that time. In Table II, we summarize the best-fit flavor fractions for each of the cases illustrated in Figs. 1 and 2, normalized as in Eq. (32). In the Appendix, we show the results assuming a μ-damped channel and combination with π-decay and neutron decay channels of varying proportions for pseudo-Dirac scenario and in those cases, the differences between the standard and pseudo-Dirac scenarios are less pronounced.

Finally, the more precise determination of several oscillation parameters in the next decade will contribute to astrophysical flavor measurements and enhance the discriminatory power of future detectors; taking into account the projected increase in precision in measurements of mixing parameters θ_{12} and θ_{23} in year 2040, the allowed regions practically shrink to best-fit points indicated by the colored circles and triangle in Figs. 1 and 2 [74].

[4]This fraction here should be understood as the detected fraction $f^{\rm det}$.

TABLE II. Flavor composition at Earth for different scenarios using the best-fit oscillation parameters of Ref. [1], assuming pion decay at the source.

At the source	
π decay	$(f_{e,S}, f_{\mu,S}, f_{\tau,S}) = (\frac{1}{3}, \frac{2}{3}, 0)$
At Earth	
Scenario	$(f^{\rm det}_{e,\oplus}, f^{\rm det}_{\mu,\oplus}, f^{\rm det}_{\tau,\oplus})$
Std. oscillations	(0.30, 0.36, 0.34)
Case 1	(0.24, 0.40, 0.36)
Case 2	(0.29, 0.36, 0.35)
Case 3	(0.36, 0.31, 0.33)
Case 12	(0.22, 0.42, 0.36)
Case 13	(0.32, 0.35, 0.33)
Case 23	(0.38, 0.30, 0.32)

V. CONCLUSIONS

In this work, we have shown that by using astrophysical neutrino flavor ratios, it is possible to distinguish between six possible cases of pseudo-Dirac neutrino spectra where there exist hierarchies among the new squared mass splitting. Our main finding is that the most sensitive cases turn out to involve the pseudo-Dirac mass splitting of the third mass eigenstates δm^2_3 which currently has the weakest constraint of the order 10^{-5} eV^2. For the cases $\delta m^2_{1,2} = 0$ or $\delta m^2_1 = 0$, a conservative upper bound of order $\delta m^2_3 \lesssim 10^{-12}$ eV^2 can be obtained considering astrophysical neutrinos of energies $E \sim 100$ TeV coming from a distance greater than the size of our galaxy and assuming π decay at neutrino sources with the IceCube-Gen2 experiment.

If nature is kind to us, we might detect the first positive evidence of pseudo-Dirac neutrino with $\delta m^2_3 \sim 10^{-12}$ eV^2 with the astrophysical neutrino flavor ratio. From Eq. (26), if extragalatic neutrino sources are determined, the bound will greatly improve, up to 5 orders of magnitude if the sources are of the distance of Gpc. The benefit of using flavor ratios is its insensitivity to absolute neutrino flux uncertainty while the main caveat is that if all pseudo-Dirac mass splittings are of the same order, one will obtain an overall reduction of flux, making this method futile. As more astrophysical neutrino sources are identified, one can combine the flavor ratio method together with direct measurements to derive the best constraints on pseudo-Dirac neutrinos, exploring completely the window of pseudo-Dirac leptogenesis proposed in Ref. [6].

Note added. A recent work [75] has also considered effects of pseudo-Dirac neutrinos on astrophysical neutrino flavor ratios and showed that if there is an overdensity of cosmic neutrino background by a factor of 10^4 around Earth, matter effect can be relevant. Since gravitational effect can only give rise to order of one enhancement, further new physics is required to achieve this large enhancement. To be conservative, we assume no such large overdensity and ignore the neutrino matter effect.

ACKNOWLEDGMENTS

Y. P. acknowledges support by Fundação de Amparo à Pesquisa do Estado de São Paulo (FAPESP) Contracts No. 2023/10734-3 and No. 2023/01467-1, and by the National Council for Scientific and Technological Development (CNPq) Grant No. 151168/2023-7. C. S. F. acknowledges support by FAPESP Contracts No. 2019/11197-6 and No. 2022/00404-3 and Conselho Nacional de Desenvolvimento Científico e Tecnológico (CNPq) under Contracts No. 407149/2021-0 and No. 304917/2023-0.

APPENDIX: μ-DAMPED PRODUCTION AND THE COMBINATION WITH π-DECAY AND NEUTRON DECAY PRODUCTION

We first show the results for the combination of μ-damped production with the pseudo-Dirac scenario. We highlight that only in Case 12 the pseudo-Dirac scenario appears as clearly distinct from standard scenarios, although it will still be hard to discriminate even after 10 yrs of IceCube-Gen2 operation. As for the pseudo-Dirac scenarios involving ν_3 mass eigenstates (Case 3, Case 13, and Case 23) assuming μ-damped sources, it can result in confusion with the standard scenario assuming π-decay sources, see Figs. 3 and 4. In Table III, we list the best-fit flavor fractions for each of the cases illustrated in Figs. 3 and 4.

TABLE III. Flavor composition at Earth for different scenarios using the best-fit oscillation parameters of Ref. [1], assuming muon damped at the source.

At the source	
μ-damped	$(f_{e,S}, f_{\mu,S}, f_{\tau,S}) = (0, 1, 0)$
At Earth	
Scenario	$(f^{\rm det}_{e,\oplus}, f^{\rm det}_{\mu,\oplus}, f^{\rm det}_{\tau,\oplus})$
Standard oscillations	(0.18, 0.45, 0.37)
Case 1	(0.16, 0.46, 0.38)
Case 2	(0.15, 0.47, 0.38)
Case 3	(0.24, 0.41, 0.35)
Case 12	(0.12, 0.49, 0.39)
Case 13	(0.24, 0.42, 0.34)
Case 23	(0.23, 0.41, 0.36)

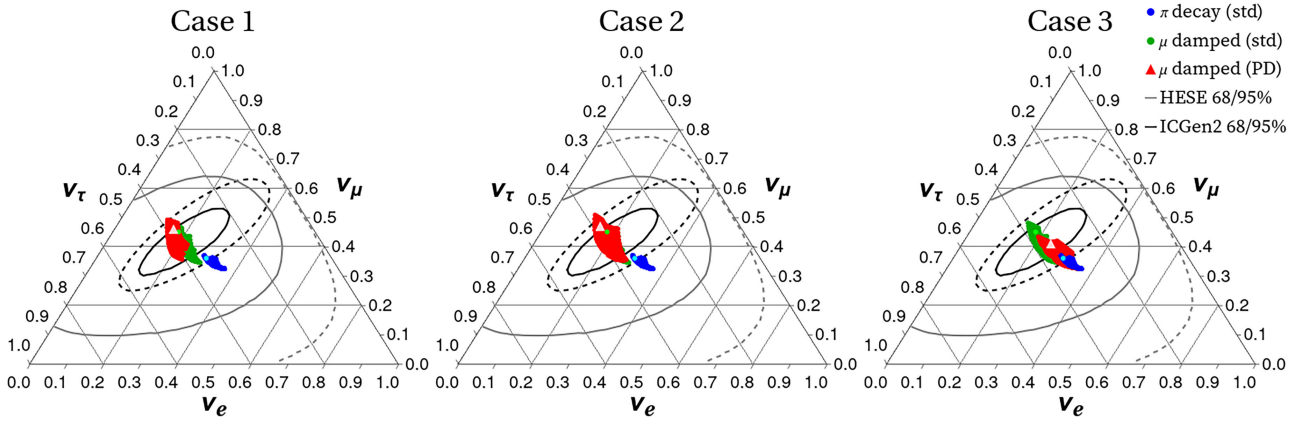


FIG. 3. Same as Fig. 1 in the main text, but with the assumption that pseudo-Dirac neutrinos are produced via the μ-damped channel and corresponding projection of IceCube-Gen2 is taken from [52].

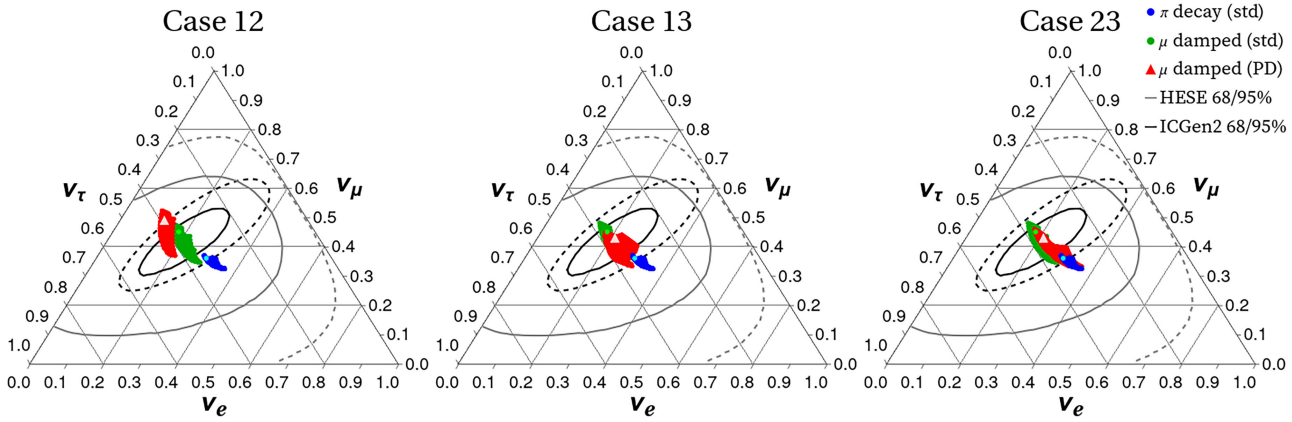


FIG. 4. Same as Fig. 2 in the main text, but with the assumption that pseudo-Dirac neutrinos are produced via the μ-damped channel and corresponding projection of IceCube-Gen2 is taken from [52].

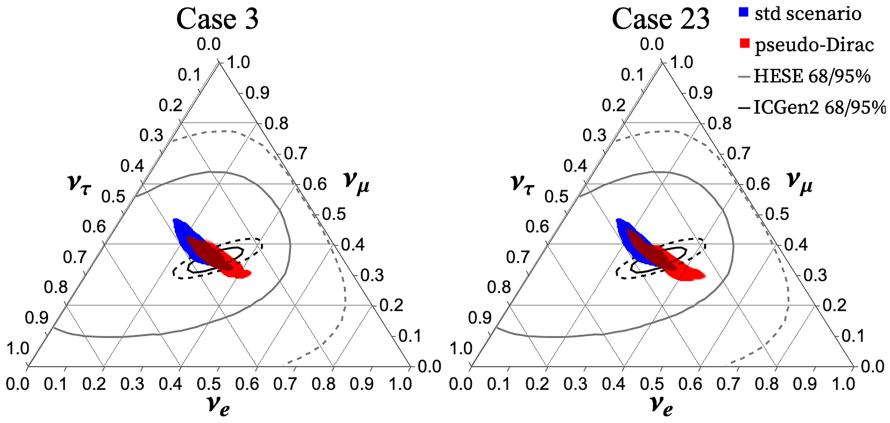


FIG. 5. Expected regions for the flavor composition of high-energy astrophysical neutrinos in the standard scenario (blue) and the pseudo-Dirac scenario (red). In both cases, we vary the oscillation parameters and consider two production mechanisms (pion decay and muon-damped) of varying proportions to obtain the allowed regions. Note that the standard and pseudo-Dirac scenarios largely overlap, except for the lower portion of the red region (originating from pion-decay sources emitting pseudo-Dirac neutrinos; see Figs. 1 and 2), which could, in principle, be distinguished by future experiments such as IceCube-Gen2.

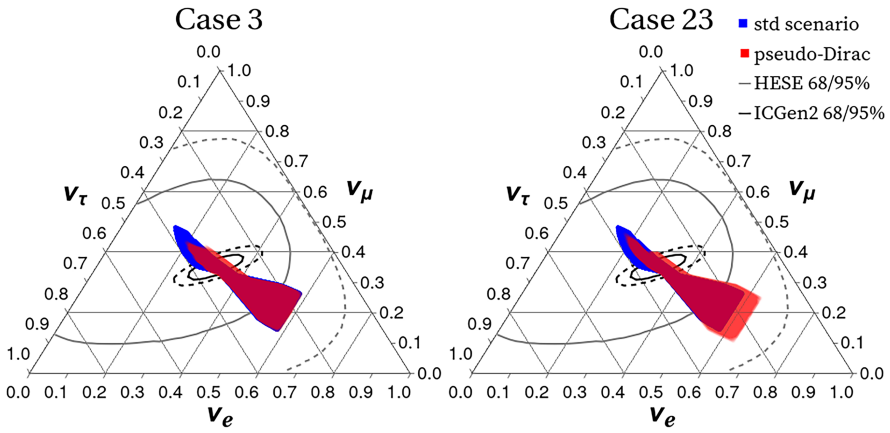


FIG. 6. Same as Fig. 5, but in addition to pion decay and muon-damped production, we include neutron decay as a possible production mechanism. Neutron decay leads to source flavor ratios of the form $(1,0,0)_S$ and corresponds to flavor ratios at Earth approximately $(0.55,0.17,0.28)_\oplus$, which pushes the allowed region toward the lower-right vertex of the flavor triangle [74].

In Fig. 5, we show ternary plots for the allowed regions in both the standard and pseudo-Dirac scenarios for the case in which π-decay and μ-damped contributions, in varying proportions, are simultaneously present. To show how this can affect the two most interesting cases (Cases 3 and 23), we present the analysis for them. The result is that corresponding regions shown in Figs. 1–4 merge significantly. The blue region corresponds to a mixture of μ-damped and π-decay contributions in varying proportions, assuming the standard scenario. It largely overlaps with the red region, which represents the same mixture but in the presence of pseudo-Dirac neutrinos (the purple or dark red region indicates the overlap between the blue and light red areas).

In Fig. 6, we add to the set of possible production processes the neutron decay, which is also a benchmark scenario often quoted in the literature. Neutron decay produces neutrinos with source flavor ratios $(1,0,0)_S$, which evolve into an approximate composition of $(0.55,0.17,0.28)_\oplus$ at Earth, thereby shifting the allowed region in the flavor triangle toward its lower-right corner in both standard and pseudo-Dirac scenarios [74].

[1] P. F. de Salas, D. V. Forero, S. Gariazzo, P. Martínez-Miravé, O. Mena, C. A. Ternes, M. Tórtola, and J. W. F. Valle, J. High Energy Phys. 02 (2021) 071.
[2] I. Esteban, M. C. Gonzalez-Garcia, M. Maltoni, T. Schwetz, and A. Zhou, J. High Energy Phys. 09 (2020) 178.
[3] G. Adhikari *et al.* (nEXO Collaboration), J. Phys. G **49**, 015104 (2022).
[4] G. Anamiati, R. M. Fonseca, and M. Hirsch, Phys. Rev. D **97**, 095008 (2018).
[5] G. Anamiati, V. De Romeri, M. Hirsch, C. A. Ternes, and M. Tórtola, Phys. Rev. D **100**, 035032 (2019).
[6] C. S. Fong, T. Gregoire, and A. Tonero, Phys. Lett. B **816**, 136175 (2021).
[7] M. Kobayashi and C. S. Lim, Phys. Rev. D **64**, 013003 (2001).
[8] M. Cirelli, G. Marandella, A. Strumia, and F. Vissani, Nucl. Phys. **B708**, 215 (2005).
[9] A. de Gouvea, W.-C. Huang, and J. Jenkins, Phys. Rev. D **80**, 073007 (2009).
[10] S. Ansarifard and Y. Farzan, Phys. Rev. D **107**, 075029 (2023).
[11] J. Franklin, Y. F. Perez-Gonzalez, and J. Turner, Phys. Rev. D **108**, 035010 (2023).
[12] R. M. Crocker, F. Melia, and R. R. Volkas, Astrophys. J. Suppl. Ser. **130**, 339 (2000).
[13] R. M. Crocker, F. Melia, and R. R. Volkas, Astrophys. J. Suppl. Ser. **141**, 147 (2002).
[14] A. Esmaili, Phys. Rev. D **81**, 013006 (2010).
[15] A. Esmaili and Y. Farzan, J. Cosmol. Astropart. Phys. 12 (2012) 014.
[16] A. S. Joshipura, S. Mohanty, and S. Pakvasa, Phys. Rev. D **89**, 033003 (2014).
[17] I. M. Shoemaker and K. Murase, Phys. Rev. D **93**, 085004 (2016).
[18] V. Brdar and R. S. L. Hansen, J. Cosmol. Astropart. Phys. 02 (2019) 023.
[19] A. De Gouvêa, I. Martinez-Soler, Y. F. Perez-Gonzalez, and M. Sen, Phys. Rev. D **102**, 123012 (2020).
[20] I. Martinez-Soler, Y. F. Perez-Gonzalez, and M. Sen, Phys. Rev. D **105**, 095019 (2022).
[21] T. Rink and M. Sen, Phys. Lett. B **851**, 138558 (2024).
[22] K. Carloni, I. Martínez-Soler, C. A. Arguelles, K. S. Babu, and P. S. B. Dev, Phys. Rev. D **109**, L051702 (2024).
[23] K. Dixit, L. S. Miranda, and S. Razzaque, arXiv:2406.06476.
[24] Y. H. Ahn, S. K. Kang, and C. S. Kim, J. High Energy Phys. 10 (2016) 092.
[25] S. Pakvasa, Mod. Phys. Lett. A **19**, 1163 (2004).
[26] C. A. Argüelles, F. Halzen, and N. Kurahashi, Phys. Rev. X **15**, 030501 (2025).
[27] M. Ahlers and F. Halzen, Prog. Part. Nucl. Phys. **102**, 73 (2018).
[28] M. G. Aartsen *et al.* (IceCube Collaboration), Phys. Rev. Lett. **111**, 021103 (2013).
[29] IceCube Collaboration, Science **342**, 1242856 (2013).
[30] M. G. Aartsen *et al.* (IceCube Collaboration), Phys. Rev. Lett. **113**, 101101 (2014).
[31] M. G. Aartsen *et al.* (IceCube Collaboration), Astrophys. J. **809**, 98 (2015).
[32] M. G. Aartsen *et al.* (IceCube Collaboration), Phys. Rev. Lett. **115**, 081102 (2015).
[33] M. G. Aartsen *et al.* (IceCube Collaboration), Astrophys. J. **833**, 3 (2016).
[34] R. Abbasi *et al.* (IceCube Collaboration), Eur. Phys. J. C **82**, 1031 (2022).
[35] R. Abbasi *et al.* (IceCube Collaboration), Phys. Rev. D **104**, 022002 (2021).
[36] R. Abbasi *et al.* (IceCube Collaboration), Astrophys. J. **928**, 50 (2022).
[37] A. Albert *et al.* (ANTARES Collaboration), Astrophys. J. Lett. **853**, L7 (2018).
[38] V. A. Allakhverdyan *et al.* (Baikal-GVD Collaboration), Phys. Rev. D **107**, 042005 (2023).
[39] M. G. Aartsen *et al.* (IceCube Collaboration), Science **361**, 147 (2018).
[40] M. G. Aartsen *et al.* (IceCube, Fermi-LAT, MAGIC, AGILE, ASAS-SN, HAWC, H.E.S.S., INTEGRAL, Kanata, Kiso, Kapteyn, Liverpool Telescope, Subaru, Swift NuSTAR, VERITAS, VLA/17B-403 Collaborations), Science **361**, eaat1378 (2018).
[41] X. Rodrigues, S. Garrappa, S. Gao, V. S. Paliya, A. Franckowiak, and W. Winter, Astrophys. J. **912**, 54 (2021).
[42] R. Abbasi *et al.* (IceCube Collaboration), Science **378**, 538 (2022).
[43] A. Albert *et al.* (ANTARES, OVRO Collaborations), Astrophys. J. **964**, 3 (2024).
[44] N. Kurahashi, K. Murase, and M. Santander, Annu. Rev. Nucl. Part. Sci. **72**, 365 (2022).
[45] S. Troitsky, Usp. Fiz. Nauk **194**, 371 (2024).
[46] M. Ahlers, Y. Bai, V. Barger, and R. Lu, Phys. Rev. D **93**, 013009 (2016).
[47] R. Abbasi *et al.* (IceCube Collaboration), Science **380**, adc9818 (2023).
[48] M. Bustamante, Nat. Rev. Phys. **6**, 8 (2024).
[49] M. Ajello *et al.*, Astrophys. J. **780**, 73 (2014).
[50] A. Capanema, A. Esmaili, and P. D. Serpico, J. Cosmol. Astropart. Phys. 02 (2021) 037.
[51] M. G. Aartsen *et al.* (IceCube-Gen2 Collaboration), J. Phys. G **48**, 060501 (2021).
[52] R. Abbasi *et al.* (IceCube-Gen2 Collaboration), Proc. Sci. ICRC2023 (**2023**) 1123 [arXiv:2308.15220].
[53] A. M. Hopkins and J. F. Beacom, Astrophys. J. **651**, 142 (2006).
[54] P. Keranen, J. Maalampi, M. Myyrylainen, and J. Riittinen, Phys. Lett. B **574**, 162 (2003).
[55] J. F. Beacom, N. F. Bell, D. Hooper, J. G. Learned, S. Pakvasa, and T. J. Weiler, Phys. Rev. Lett. **92**, 011101 (2004).
[56] N. Aghanim *et al.* (Planck Collaboration), Astron. Astrophys. **641**, A6 (2020); **652**, C4(E) (2021).
[57] S. Paiano, M. Landoni, R. Falomo, A. Treves, R. Scarpa, and C. Righi, Astrophys. J. **837**, 144 (2017).
[58] S. H. Margolis, D. N. Schramm, and R. Silberberg, Astrophys. J. **221**, 990 (1978).
[59] F. W. Stecker, Astrophys. J. **228**, 919 (1979).
[60] A. Mucke, R. Engel, J. P. Rachen, R. J. Protheroe, and T. Stanev, Comput. Phys. Commun. **124**, 290 (2000).
[61] S. R. Kelner, F. A. Aharonian, and V. V. Bugayov, Phys. Rev. D **74**, 034018 (2006); **79**, 039901(E) (2009).
[62] S. Hummer, M. Ruger, F. Spanier, and W. Winter, Astrophys. J. **721**, 630 (2010).

[63] S. L. Glashow, Phys. Rev. **118**, 316 (1960).
[64] A. Bhattacharya, R. Gandhi, W. Rodejohann, and A. Watanabe, J. Cosmol. Astropart. Phys. 10 (2011) 017.
[65] G.-y. Huang, M. Lindner, and N. Volmer, J. High Energy Phys. 11 (2023) 164.
[66] Q. Liu, N. Song, and A. C. Vincent, Phys. Rev. D **108**, 043022 (2023).
[67] IceCube Collaboration, Nature (London) **591**, 220 (2021); **592**, E11 (2021).
[68] J. P. Rachen and P. Meszaros, Phys. Rev. D **58**, 123005 (1998).
[69] T. Kashti and E. Waxman, Phys. Rev. Lett. **95**, 181101 (2005).
[70] M. Kachelriess, S. Ostapchenko, and R. Tomas, Phys. Rev. D **77**, 023007 (2008).
[71] S. Hummer, M. Maltoni, W. Winter, and C. Yaguna, Astropart. Phys. **34**, 205 (2010).
[72] W. Winter, Phys. Rev. D **90**, 103003 (2014).
[73] P. S. B. Dev, S. Jana, and Y. Porto, arXiv:2312.17315.
[74] N. Song, S. W. Li, C. A. Argüelles, M. Bustamante, and A. C. Vincent, J. Cosmol. Astropart. Phys. 04 (2021) 054.
[75] P. S. B. Dev, P. A. N. Machado, and I. Martinez-Soler, Phys. Lett. B **862**, 139306 (2025).